Journal of Sound and Vibration (2001) **248**(3), 521–532
doi:10.1006/jsvi.2001.3834, available online at http://www.idealibrary.com on IDEAL®

CHAOTIC MOTION IN THE GENERIC SEPARATRIX BAND OF A MATHIEU–DUFFING OSCILLATOR WITH A TWIN-WELL POTENTIAL

A. C. J. Luo

Department of Mechanical and Industrial Engineering, Southern Illinois University at Edwardsville, Edwardsville, IL 62026-1805 *U.S.A. E-mail: aluo@siue.edu*

(*Received* 20 *November* 2000, *and in final form* 14 *May* 2001)

The resonant conditions for the Mathieu–Duffing oscillator are determined, and the resonant orders for the inside and outside of the generic separatrix are $(M:1)$ and $(2M:1)$ respectively. The excitation strength for the onset of a specific resonance in the generic separatrix band is predicted analytically and numerically through the incremental energy approach and the energy spectrum methods. For comparison of the separatrix splitting theory, the widths of the generic separatrix band are computed through the maximum and minimum energies. The bandwidth is not linear to the excitation strength, and it is strongly dependent on the resonance. The results can be applied to the post-buckled structures under parametric excitation forces. However, the chaotic motion in the resonant separatrix band needs to be investigated for a better understanding of chaotic motion in the Mathieu–Duffing oscillator.

© 2001 Academic Press

1. INTRODUCTION

Consider a Mathieu–Duffing oscillatory with a twin-well potential

$$\ddot{x} - [\alpha_1 + Q_0 \cos(\Omega t)]x + \alpha_2 x^3 = 0, \tag{1}$$

where $\alpha_1 > 0$ and $\alpha_2 > 0$ are system parameters, Q_0 and Ω are the excitation strength and frequency respectively. The above equation can be derived from the buckled structures under the longitudinal, periodic forces through the Galerkin method. The system parameters α_1 and α_2 are linear (relevant to buckling load and bending moment) and non-linear terms (relevant to longitudinal internal normal forces). To point out the engineering significance of equation (1), a simply supported, initially straight, slender rod experiencing large deformation subjected to an axially compressive force $P + P_0 \cos \Omega t$ at one end, shown in Figure 1, is considered as an example for illustration.

The time-independent H_0 (unperturbed) and time-dependent H_1 (perturbation) in the Hamiltonian of equation (1) are

$$H_0 = \tfrac{1}{2}\dot{x}^2 - \tfrac{1}{2}\alpha_1 x^2 + \tfrac{1}{4}\alpha_2 x^4, \; H_1 = -\tfrac{1}{2}x^2 Q_0 \cos(\Omega t). \tag{2}$$

For the unperturbed system of equation (1), there are two homoclinic separatrices related to the saddle point (0, 0) for $H_0 = E_0 = 0$. Such two generic separatrices separates the motions of the unperturbed Mathieu–Duffing oscillator into inside and outside periodic motions. Hence, under a periodic excitation, the resonant characteristics of chaotic motions inside

0022-460X/01/480521 + 12 $35.00/0 © 2001 Academic Press

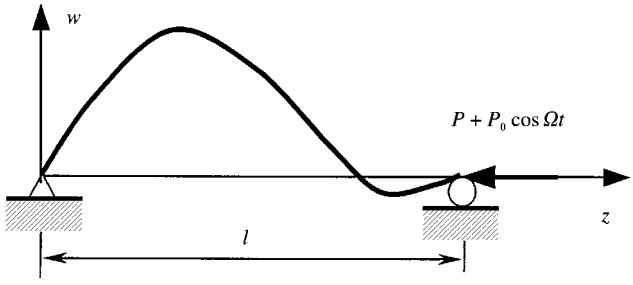

Figure 1. A non-linear, planar rod subjected to the compressive force $P + P_0 \cos \Omega t$.

and outside the generic separatrix of the Mathieu–Duffing oscillator are distinguishing themselves. The motion bands associated with the separatrix inside and outside regions are termed the inner and outer separatrix bands respectively. In this paper, the resonance-characterized chaotic motion in the separatrix band of the Mathieu–Duffing oscillator will be investigated.

The Duffing oscillator as a typical example in mechanical systems has been extensively investigated (e.g., reference [1]) since Duffing [2] investigated the dynamic behavior of such a non-linear oscillatory system in 1918. The non-linear behavior of the Duffing oscillator with week non-linearity was further investigated through the perturbation approach. However, the perturbation analysis only gave the local non-linear behavior. For strong non-linearity, the non-linear behaviors of Duffing oscillators with periodic excitation are still not clear. For instance, the resonance characterization of chaotic motion in the Duffing oscillators is still unsolved, although one used the zero of the Melnikov function to predict the onset of such a motion in simple systems. This oscillator was also used to describe the motion of a particle trapped in double-well potential in the presence of a monochronic external force field [3]. In 1984, Reichl and Zheng [3, 4] used standard mapping, the Chirikov overlap [5] and renormalization approaches [6] to investigate such chaotic motion of the particle trapped in a double-well potential. In 1999, Luo and Han [7] modified the Chirikov overlap approach and improved the standard mapping approach to predict the resonant characterization of chaotic motion in the Duffing oscillator. Luo *et al.* [8] developed a numerical approach to predict the onset of resonance in chaotic motions in the separatrix band (or the stochastic layer) in the periodically driven twin-well Duffing oscillator. In 2000 Luo [9] developed an accurate standard mapping approach for the analytical prediction of the appearance of resonance in such a layer, and Luo and Han [10] also developed the incremental energy approach to analytically predict the appearance and disappearance of the resonance in the chaotic motions. However, all the cases for the Duffing oscillators are based on the forced vibration. The resonant characterization of the Duffing oscillator under a parametric excitation was not investigated.

From linear parametric oscillations [11–13], the vibration responses are different from the forced vibration. In 1965, Tso and Caughey [14] investigated the parametric vibration of a non-linear system through the slowly varying parameter technique, and in 1993, Mond *et al.* [15] gave the stability analysis of non-linear Mathieu equation through the normal form technique. However, the normal forms are obtained through the simplification of analytical expression of the vector field on the center manifold. Such a simplification leads to the normal form technique only applicable for a qualitative analysis of the vector flow near bifurcation only. Therefore, such a technique cannot further be used to predict chaotic motions in parametric oscillators. The quasi-periodic Mathieu oscillators were also investigated recently (e.g., references [16, 17]). In reference [17], the spectral balance

method was used to get the frequency response solutions, but the analytical prediction of chaotic motion in such oscillators was not given. From the literature survey, the chaotic motion close to the region of the separatrix needs to be investigated.

In this paper, the conditions for the onset of primary resonance in the chaotic motion of the Mathieu–Duffing oscillator will be obtained. The numerical prediction for the appearance of the specified primary resonance in the separatrix band will be completed though the energy spectrum. The width of chaotic motion band near the separatrix is also computed. The analytical condition for the onset of the specified primary resonance in the separatrix band will be developed, and numerical simulations will be carried out to demonstrate the resonant characteristics of chaotic motion in the separatrix band.

2. INNER SEPARATRIX BAND

For the given energy E_α satisfying $H_0 = E_\alpha < E_0$, the solution of the inner orbit without the excitation in references [8, 18, 19] is

$$x_\alpha^{(0)} = \pm e_\alpha \, \mathrm{d}n\left[\frac{K(k_\alpha)\omega_\alpha t}{\pi}, k_\alpha\right], \tag{3}$$

where dn is the Jacobi-elliptic functions, $K(k)$ the complete elliptic integral of the first kind and k the modulus of the Jacobi-elliptic function, and the subscript α denotes the inside of separatrix. The modulus k_α, the response amplitude e_α and the natural frequency ω_α are

$$k_\alpha = \sqrt{\frac{2\sqrt{\alpha_1^2 + 4\alpha_2 E_\alpha}}{\alpha_1 + \sqrt{\alpha_1^2 + 4\alpha_2 E_\alpha}}}, \quad e_\alpha = \sqrt{\frac{2\alpha_1}{(2 - k_\alpha^2)\alpha_2}}, \quad \omega_\alpha = \frac{\sqrt{\alpha_2}\, e_\alpha \pi}{\sqrt{2} K(k_\alpha)}. \tag{4}$$

Using the unperturbed solution in equation (3) to approximate the perturbed one, the total energy becomes

$$H = H_0(x, y) - \tfrac{1}{2} x^2 Q_0 \cos(\Omega t) \approx E_\alpha - \tfrac{1}{2}(x_\alpha^{(0)})^2 Q_0 \cos(\Omega t). \tag{5}$$

As in references [18, 19], substitution of equation (3) into equations (5) and expansion of the time-dependent term give

$$H \approx E_\alpha - \frac{\pi^2 e_\alpha^2 Q_0}{4K^2}\left\{\frac{1}{2}\cos\Omega t + \sum_{M=1}^{\infty}\left[p_M + \frac{1}{2}\sum_{m=1}^{\infty}\sum_{n=1}^{\infty}(p_m p_n \delta_{m+n}^M + p_m p_n \delta_{|m-n|}^M)\right]\right.$$
$$\left.\times\,[\cos(M\omega_\alpha - \Omega)t + \cos(M\omega_\alpha + \Omega)t]\right\}, \tag{6}$$

where

$$p_i = \operatorname{sech}\left[\frac{i\pi K'}{K}\right] \quad \text{and} \quad K'(k_\alpha) = K(k'_\alpha),\ k'_\alpha = \sqrt{1 - k_\alpha^2}, \quad i = \{m, n\}. \tag{7}$$

From equation (6), the resonant condition in reference [18] is

$$M\omega_\alpha = \Omega. \tag{8}$$

Note that the resonance relative to $m\omega = n\Omega$ is termed the $(m:n)$ resonance. From the traditional perturbation analysis, the resonant condition is $2M\omega_\alpha = \Omega$ because such

a perturbation analysis is based on a linear equation (i.e., the linear Mathieu equation). The corresponding stability based on the linearized equation (Mathieu equation) may not exist.

The twin-well Duffing oscillator has two potential wells. As in reference [5], the mapping for investigation of chaotic motion will be developed through the energy and phase changes for each period. The energy change in the two wells along the inner $(M:1)$ resonant orbit is approximated [5, 18] by

$$\Delta H_0^{\alpha}(\varphi_i) = 2\int_{t_i}^{T_\alpha + t_i} (f_1 g_2 - f_2 g_1)\,\mathrm{d}t \approx 2\int_{t_i}^{T_\alpha + t_i} x_\alpha^{(0)} y_\alpha^{(0)} Q_0 \cos(\Omega t)\,\mathrm{d}t = 2Q_0 Q_\alpha^{(M:1)} \sin\varphi_i, \quad (9)$$

where $\varphi_i = \Omega t_i$ and

$$\begin{aligned} f_1 &= y = \dot{x}, \quad g_1 = \alpha_1 x - \alpha_2 x^3, \\ f_2 &= 0, \quad g_2 = x Q_0 \cos\Omega t, \end{aligned} \quad (10)$$

$$Q_\alpha^{(M:1)} = \frac{\pi^2 \Omega}{K\alpha_2}\sqrt{\frac{\alpha_1}{2-k^2}}\left[p_M + \frac{1}{2}\sum_{m=1}^{\infty}\sum_{n=1}^{\infty}(p_m p_n \delta_{m+n}^{M} + p_m p_n \delta_{|m-n|}^{M})\right]. \quad (11)$$

The phase change is from equation (4):

$$\Delta\varphi^{\alpha}(E_\alpha) = \frac{2\pi\Omega}{\omega_\alpha} = \frac{2\Omega\sqrt{2-k_\alpha^2}K(k_\alpha)}{\sqrt{\alpha_1}}. \quad (12)$$

Therefore, from equation (9) and phase change, the accurate whisker map for the inner band of the Mathieu–Duffing oscillator is

$$E_\alpha^{(i+1)} - E_\alpha^{(i)} \approx 2Q_0 Q_\alpha^{(M:1)} \sin\varphi_i,\ \varphi_{i+1} - \varphi_i = \frac{2\pi\Omega}{\omega_\alpha} = \frac{2\Omega\sqrt{2-(k_\alpha)^2}K(k_\alpha)}{\sqrt{\alpha_1}}. \quad (13)$$

When $\varphi_{i+1} - \varphi_i = \varphi_{i+1}^{(M:1)} - \varphi_i^{(M:1)} = 2M\pi$, from the second one of equation (13), we can compute $k_\alpha^{(M:1)}$ from which $E_\alpha^{(M:1)}$ can be obtained from equation (4). If $E_\alpha^{(i+1)} = E_\alpha^{(i)} = E_\alpha^{(M:1)}$, we obtain $\varphi_i^{(M:1)} = 0, \pi$. As in reference [9], using the energy and phase relative to the $(M:1)$-resonance leads to a standard map if $w_i = E_\alpha^{(i+1)} - E_\alpha^{(M:1)}$ and $\phi_i = \varphi_i - \varphi_i^{(M:1)}$, i.e.,

$$w_{i+1} = w_i + D\sin\phi_i \quad \text{and} \quad \phi_{i+1} \approx \phi_i + w_{i+1}, \quad (14)$$

where $G_\alpha^{(m_\alpha:n_\beta)}\Delta H_0^{\alpha}(\varphi_i) = D\sin\varphi_i$ and $G_\alpha^{(M:1)} = \partial\Delta\varphi^{\alpha}/\partial E_\alpha|_{E_\alpha = E_\alpha^{(M:1)}}$. For the foregoing, the strength of the stochasticity parameter is $D = D^* \approx 0{\cdot}9716\cdots$ in references [20, 21] for the transition to global stochasticity in equation (14). Therefore, the excitation strength for the onset of a specific resonance in the inner separatrix band is approximately computed through

$$Q_0 \approx \frac{0{\cdot}4858}{Q_\alpha^{(M:1)} G_\alpha^{(M:1)}}, \quad (15)$$

where

$$G_\alpha^{(M:1)} = -\frac{\Omega\alpha_2[2-(k_\alpha^{(M:1)})^2]^{5/2}}{(k_\alpha^{(M:1)})^4\,\alpha_1^2\sqrt{\alpha_1}}\left\{2K(k_\alpha^{(M:1)}) - \frac{2-(k_\alpha^{(M:1)})^2}{1-(k_\alpha^{(M:1)})^2}E(k_\alpha^{(M:1)})\right\}. \quad (16)$$

From equation (12), due to $E_0 = 0$, the incremental energy approach [10] gives the approximate condition for the onset of resonance in the inner separatrix band as

$$Q_0 = \frac{|E_\alpha^{(M:1)} - E_0|}{2Q_\alpha^{(M:1)}} = \frac{|E_\alpha^{(M:1)}|}{2Q_\alpha^{(M:1)}}. \tag{17}$$

3. OUTER SEPARATRIX BAND

In a same manner, for the given energy E_β satisfying $H_0 = E_\beta > E_0$, the solution of the outer orbit [8, 18] is

$$x_\beta^{(0)} = e_\beta \mathrm{cn}\left[\frac{2K(k_\beta)\omega_\beta t}{\pi}, k_\beta\right]. \tag{18}$$

The modulus k_β, the response amplitude e_β, and the natural frequency ω_β are

$$k_\beta = \sqrt{\frac{\alpha_1 \pm \sqrt{\alpha_1^2 + 4\alpha_2 E_\beta}}{2\sqrt{\alpha_1^2 + 4\alpha_2 E_\beta}}}, \quad e_\beta = \sqrt{\frac{2k_\beta^2 \alpha_1}{(2k_\beta^2 - 1)\alpha_2}}, \quad \omega_\beta = \frac{\sqrt{\alpha_2} e_\beta \pi}{2\sqrt{2} k_\beta K(k_\beta)}. \tag{19}$$

Substitution of equation (18) into equation (2) and expansion of the time-dependent term gives the total energy

$$\begin{aligned} H &\approx E_\beta - \frac{1}{2}(x_\beta^{(0)})^2 Q_0 \cos(\Omega t) \\ &= E_\beta - \frac{\pi^2 e_\beta^2 Q_0}{8k_\beta^2 K^2} \sum_{M=1}^{\infty} \sum_{m=1}^{\infty} \sum_{n=1}^{\infty} (q_{2m-1} q_{2n-1} \delta_{2(m+n-1)}^{2M} + q_{2m-1} q_{2n-1} \delta_{2|m-n|}^{2M}) \\ &\quad \times [\cos(2M\omega_\beta - \Omega)t + \cos(2M\omega_\beta + \Omega)t], \end{aligned} \tag{20}$$

where

$$q_i = \mathrm{sech}\left[\left(i - \frac{1}{2}\right)\frac{\pi K'}{K}\right] \quad \text{and} \quad K'(k_\beta) = K(k'_\beta), \quad k'_\beta = \sqrt{1 - k_\beta^2}, \quad i = \{m, n\}. \tag{21}$$

From equation (20), the resonant condition is

$$2M\omega_\beta = \Omega \tag{22}$$

different from the inner resonance in equation (8). In a similar fashion, the energy increment along the outer $(2M{:}1)$ resonant orbit is computed through

$$\Delta H_0^\beta(\varphi_i) \approx \int_{t_i}^{T_\alpha + t_i} x_\beta^{(0)} y_\beta^{(0)} Q_0 \cos(\Omega t)\, \mathrm{d}t = Q_0 Q_\beta^{(2M:1)} \sin\varphi_i \tag{23}$$

and

$$Q_\beta^{(2M:1)} = \frac{\pi^2 \Omega}{K\alpha_2} \sqrt{\frac{\alpha_1}{2k_\beta^2 - 1}} \sum_{m=1}^{\infty} \sum_{n=1}^{\infty} (q_{2m-1} q_{2n-1} \delta_{2(m+n-1)}^{2M} + q_{2m-1} q_{2n-1} \delta_{2|m-n|}^{2M}). \tag{24}$$

The phase change is, from equation (19),

$$\Delta\varphi^{\beta}(E_{\beta}) = \frac{2\pi\Omega}{\omega_{\beta}} = \frac{4\Omega K(k_{\beta})\sqrt{2k_{\beta}^2 - 1}}{\sqrt{\alpha_1}}. \tag{25}$$

Therefore, from equation (23) and phase change, the accurate whisker map for the outer band of the Mathieu–Duffing oscillator is

$$E_{\beta}^{(i+1)} - E_{\beta}^{(i)} \approx Q_0 Q_{\beta}^{(2M:1)} \sin\varphi_i, \varphi_{i+1} - \varphi_i = \frac{2\pi\Omega}{\omega_{\beta}} = \frac{4\Omega\sqrt{2(k_{\alpha})^2 - 1K(k_{\beta})}}{\sqrt{\alpha_1}}. \tag{26}$$

The excitation strength for the onset of the $(2M{:}1)$-resonance in the outer separatrix band is computed from the accurate standard mapping approach

$$Q_0 \approx \frac{0{\cdot}9716}{Q_{\beta}^{(2M:1)} G_{\beta}^{(2M:1)}}, \tag{27}$$

where

$$G_{\beta}^{(2M:1)} = \frac{2\Omega\alpha_2 [2(k_{\beta}^{(2M:1)})^2 - 1]^{5/2}}{(k_{\beta}^{(2M:1)})^2 \alpha_1^2 \sqrt{\alpha_1}} \left[K(k_{\beta}^{(2M:1)}) - \frac{1 - 2(k_{\beta}^{(2M:1)})^2}{1 - (k_{\beta}^{(2M:1)})^2} E(k_{\beta}^{(2M:1)}) \right]. \tag{28}$$

The incremental energy approach gives the approximate condition for the onset of the $(2M{:}1)$-resonance in the outer separatrix band

$$Q_0 = \frac{|E_{\beta}^{(2M:1)} - E_0|}{Q_{\beta}^{(2M:1)}} = \frac{|E_{\beta}^{(2M:1)}|}{Q_{\beta}^{(2M:1)}}. \tag{29}$$

4. ENERGY SPECTRUM

Before the energy spectrum is computed, the averaging of the Hamiltonian energy is discussed herein. For the inner separatrix band, except for the term of the $(M{:}1)$-resonance, all other terms in H in equation (6) will average to zero over one period ($T_{\alpha} = 2\pi/\omega_{\alpha}$). The averaging of the Hamiltonian for the $(M{:}1)$ primary resonance (i.e., $M\omega_{\alpha} = \Omega$) is strongly dependent on the resonance order, and its magnitude $\bar{H}$ in the inner separatrix band for the specific resonance is

$$\bar{H} \approx \frac{\pi^2 e_{\alpha}^2 Q_0}{4K^2} \left[p_M + \frac{1}{2} \sum_{m=1}^{\infty} \sum_{n=1}^{\infty} (p_m p_n \delta_{m+n}^{M} + p_m p_n \delta_{|m-n|}^{M}) \right]. \tag{30}$$

For the outer separatrix, the averaging of the Hamiltonian for the $(2M{:}1)$ primary resonance (i.e., $2M\omega_{\beta} = \Omega$) gives the magnitude $\bar{H}$ in the outer separatrix band:

$$\bar{H} \approx \frac{\pi^2 e_{\beta}^2 Q_0}{8k_{\beta}^2 K^2} \sum_{m=1}^{\infty} \sum_{n=1}^{\infty} (q_{2m-1} q_{2n-1} \delta_{2(m+n-1)}^{2M} + q_{2m-1} q_{2n-1} \delta_{2|m-n|}^{2M}). \tag{31}$$

However, the averaging of the Hamiltonian energy is zero for non-resonant responses. Equations (30) and (31) indicate that the Hamiltonian energy will undergo a large change when the specific resonance is involved in the separatrix band, and the averaging of the

Hamiltonian for the different resonance is different. In addition, the two averaged Hamiltonian energies for the inner and outer separatrix bands are distinguishing as well.

Luo *et al.* [8] developed the energy spectrum approach for the numerical prediction of the onset of the resonance in the stochastic layer (or the separatrix band). Therefore, such an energy spectrum approach is used for determining the critical value of excitation frequency for a given excitation strength. This energy spectrum is based on the energy of the Poincaré mapping points of the separatrix band. The Poincaré mapping points for the Mathieu–Duffing oscillator are defined through the Poincaré section:

$$\Sigma = \left\{ (x(t_N), \dot{x}(t_N)) \,\middle|\, \text{satisfying equation (1), and } t_N = \frac{2N\pi}{\Omega} + t_0,\ N = 0, 1, \ldots \right\}, \tag{32}$$

where $x(t_N) = x_N$, $\dot{x}(t_N) = \dot{x}_N$ and the initial conditions are $x(t_0) = x_0$, $\dot{x}(t_0) = \dot{x}_0$ at $t = t_0$. The Poincaré map is $P: \Sigma \to \Sigma$. The conservative energy of Mathieu–Duffing oscillator for the Nth iteration Poincaré mapping point is computed through

$$H_0^{(N)} = \tfrac{1}{2}\dot{x}_N^2 - \tfrac{1}{2}\alpha_1 x_N^2 + \tfrac{1}{4}\alpha_2 x_N^4 \tag{33}$$

and the corresponding minimum and maximum energies are obtained:

$$E_{max} = \max_{N \to \infty} \{H_0^{(N)}\} \quad \text{and} \quad E_{min} = \min_{N \leftarrow \infty} \{H_0^{(N)}\}. \tag{34}$$

Using the above definition, the maximum and minimum energy spectra are shown in Figure 2(a) for $Q_0 = 0{\cdot}1$ and $\alpha_1 = \alpha_2 = 1{\cdot}0$ in equation (1). The maximum and minimum energies are computed from 10 000 iterations of Poincaré map for each excitation frequency. $\Omega^{\alpha(M:1)}$ (or $\Omega^{\beta(M:1)}$) denotes a maximum value of excitation frequency when the $(M:1)$-inner inner (or $(2M:1)$-outer) resonance disappears in the separatrix band. The energy jumps occur at $\Omega^{\beta(2:1)} \approx 2{\cdot}15$, $\Omega^{\beta(4:1)} \approx 3{\cdot}3$, $\Omega^{\beta(6:1)} \approx 3{\cdot}95$, $\Omega^{\beta(8:1)} \approx 4{\cdot}55$ for the outer separatrix band and, at $\Omega^{\alpha(2:1)} \approx 2{\cdot}60$ and $\Omega^{\alpha(3:1)} \approx 3{\cdot}5$, $\Omega^{\alpha(4:1)} \approx 4{\cdot}30$, $\Omega^{\alpha(5:1)} \approx 4{\cdot}85$ for the inner separatrix band. These specific values are critical excitation frequencies for the disappearance of the specific resonance in the separatrix band. Note that for $Q_0 = 0{\cdot}1$, the resonant-separatrix of the first order in the inner separatrix band cannot be observed because the Hamiltonian

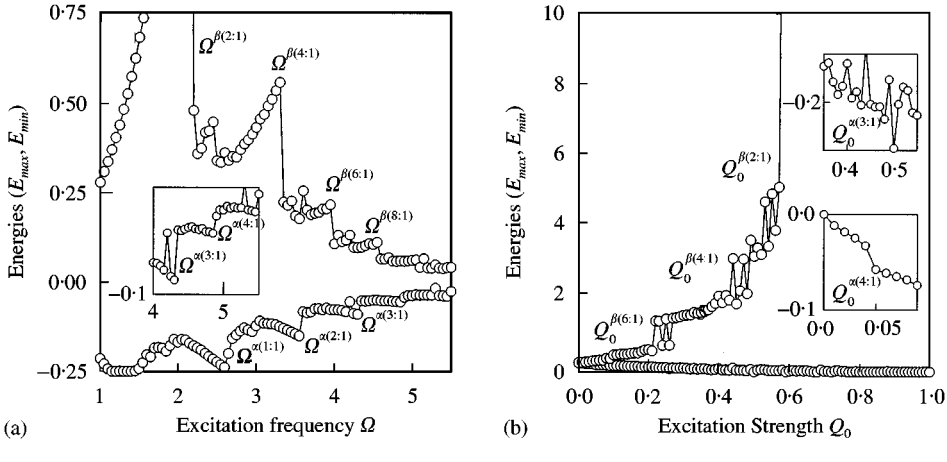

Figure 2. Minimum and maximum energy spectra of the separatrix band (a) $Q_0 = 0{\cdot}1$ and (b) $\Omega = 4$ in the Mathieu–Duffing oscillator $\alpha_1 = \alpha_2 = 1{\cdot}0$.

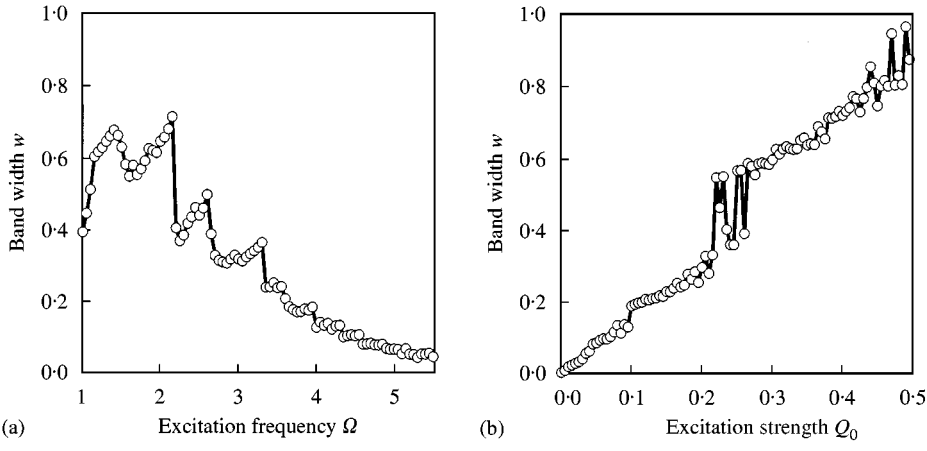

Figure 3. The bandwidth varying with excitation frequency and strength: (a) $Q_0 = 0{\cdot}1$ and (b) $\Omega = 4$ for the separatrix band of the Mathieu–Duffing oscillator ($\alpha_1 = \alpha_2 = 1{\cdot}0$).

arrives at the minimum energy $-0{\cdot}25$ (for $\alpha_1 = \alpha_2 = 1{\cdot}0$) until this resonant-separatrix appears. To interpret the critical values, consider $\Omega > \Omega^{\beta(6:1)} \approx 3{\cdot}95$ at $Q_0 = 0{\cdot}1$, the lower than (6:1)-outer resonance in the outer band will not appear, and the lower than (3:1)-inner resonance in the inner-band will not appear as well because of $\Omega > \Omega^{\beta(6:1)} > \Omega^{\alpha(3:1)}$. For further illustration of the energy change in the separatrix band, the minimum and maximum energies varying with excitation strength are presented in Figure 2(b) for $\Omega = 4$, the critical values for the appearance of the specific resonance are $Q_0^{\beta(6:1)} \approx 0{\cdot}22$, $Q_0^{\beta(4:1)} \approx 0{\cdot}44$, $Q_0^{\beta(2:1)} \approx 0{\cdot}58$ and $Q_0^{\alpha(4:1)} \approx 0{\cdot}05$, $Q_0^{\alpha(5:1)} \approx 0{\cdot}48$.

In 1890, Poincare [22] investigated the splitting of the separatrix in non-linear Hamiltonian system. Since then, the layer width was estimated qualitatively through the perturbation theory (e.g., references [22–24]). Using the definition of the layer width in reference [8], the separatrix bandwidth is computed through

$$w \equiv \min_{t \in [0,\ \infty)} \|\mathbf{x}(E^{max}, t) - \mathbf{x}(E^{min}, t)\| \equiv \|\mathbf{x}^{max} - \mathbf{x}^{min}\|, \tag{35}$$

where $\|\bullet\|$ is a norm. The detail for the bandwidth was given in reference [8]. For the Duffing-related oscillator, the separatrix bandwidth is $|\mathbf{x}^{max} - \mathbf{x}^{min}|$ at $y = 0$ which can be determined numerically. Based on the minimum and maximum energies in Figure 2, the corresponding bandwidths are computed, as shown in Figure 3. These indicate that the bandwidth is strongly dependent on the resonance order, and not linear to either excitation frequency or excitation strength. Such a solution shows that the qualitative results in references [22–25] may not be true because those analyses were based on perturbation and linearization.

5. COMPARISON

To compare the analytical predictions with the numerical ones of the onset of resonance in the separatrix band, the resonant conditions are illustrated in Figure 4 through the excitation frequency versus the unperturbed Hamiltonian energy, where the order of the resonance in the inner and outer bands are clearly demonstrated. When the conservative energy is given, the excitation frequency for a specific resonance can be determined.

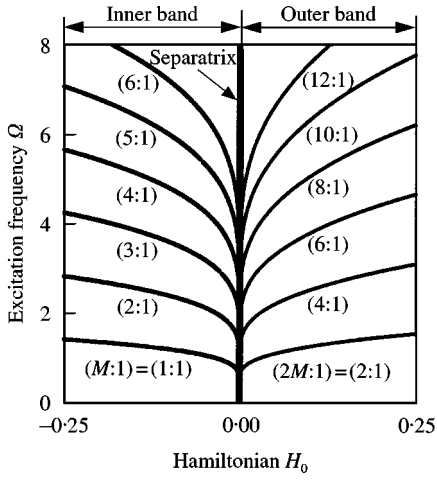

Figure 4. The resonant conditions for the separatrix band of the Mathieu–Duffing oscillator ($\alpha_1 = \alpha_2 = 1{\cdot}0$).

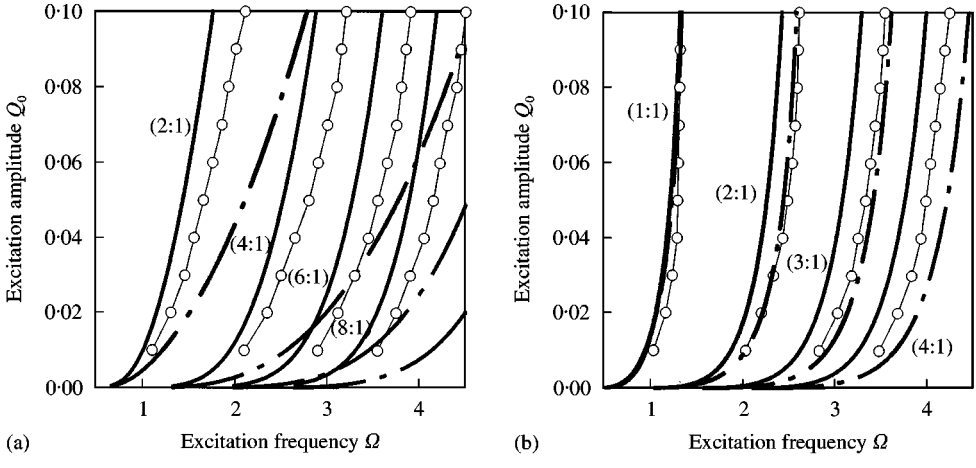

Figure 5. Conditions for the onset of a specific resonance in (a) the outer band and (b) the inner band of the Mathieu–Duffing oscillator with *weak* excitation ($\alpha_1 = \alpha_2 = 1{\cdot}0$) ———, incremental energy; – – – –, standard mapping; ○—○—, numerical.

The numerical and analytical predictions of excitation strengths for the weak and strong excitation are illustrated in Figures 5 and 6 respectively. The solid and dashed curves denote the analytical predictions based on the incremental energy approach and accurate standard map method, and the hollow circle curve represents the numerical predictions based on the energy spectrum approach. The incremental energy approach gives a good prediction for week excitation compared to the numerical prediction. However, such a prediction for strong excitation, illustrated in Figure 6, becomes worse because the sub-resonance effect is not considered in the incremental energy approach and the energy increments are approximately computed through the unperturbed orbits rather than the perturbed ones. The accurate standard mapping approach gives a poor prediction for the resonance in the separatrix band of Mathieu–Duffing oscillator because of linearization of accurate whicker mapping in the period-1 of the specified resonance.

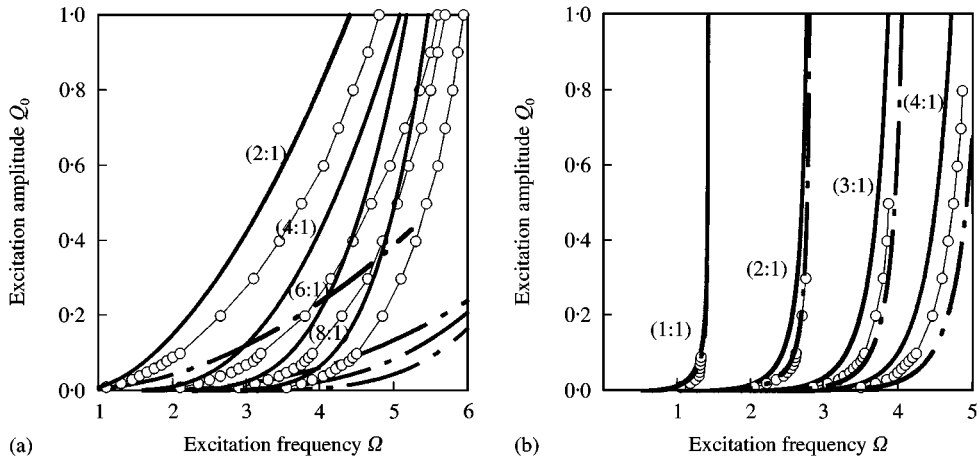

Figure 6. Conditions for the onset of a specific resonance in (a) the outer band and (b) the inner band of the Mathieu–Duffing oscillator with strong excitation ($\alpha_1 = \alpha_2 = 1{\cdot}0$) ———, incremental energy; – – – –, standard mapping; ○—○—, numerical.

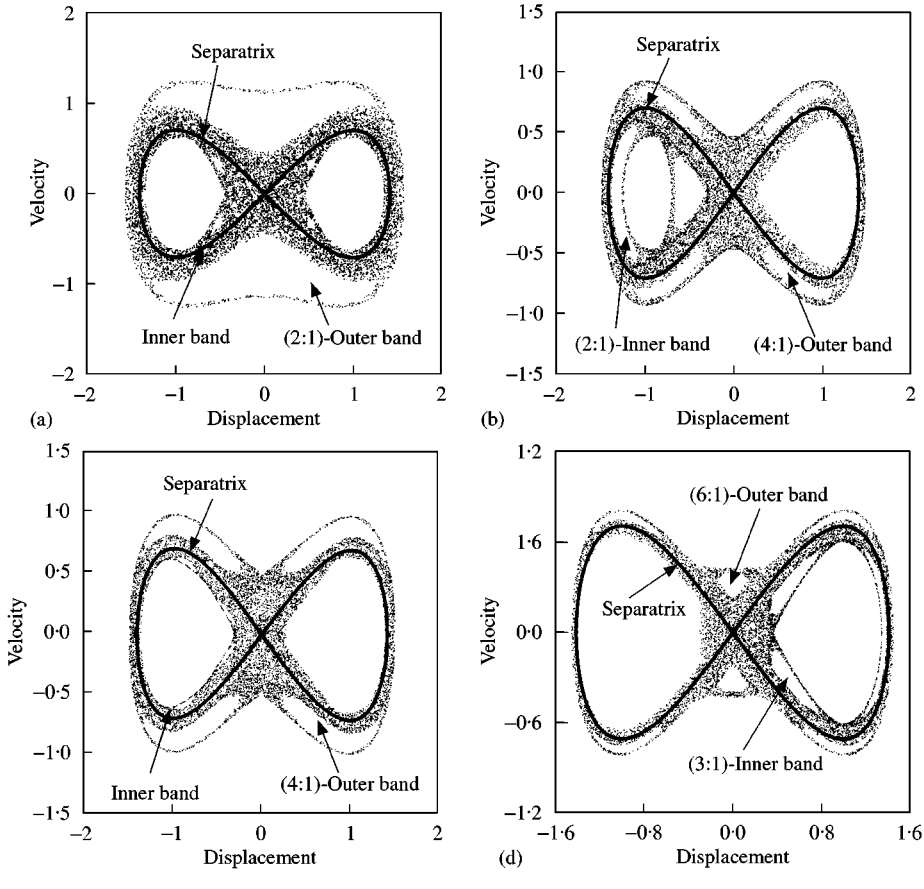

Figure 7. Poincaré mapping sections of the chaotic motion of the Mathieu–Duffing oscillator at ($\alpha_1 = \alpha_2 = 1$, $Q_0 = 0{\cdot}05$): (a) the (2:1)-resonance in the outer band ($\Omega = 1{\cdot}65$ less than and close to $\Omega_{cr}^{\beta(2:1)}$), (b) the (4:1)-resonance and (2:1)-resonance in the outer and inner bands ($\Omega = 2{\cdot}45$ less than and close to $\Omega_{cr}^{\alpha(2:1)}$ and $\Omega_{cr}^{\beta(4:1)}$), (c) the (4:1)-resonance in the outer band ($\Omega = 2{\cdot}7$ less than and close to $\Omega_{cr}^{\beta(4:1)}$), and (d) the (6:1)-resonance and (3:1)-resonance in the outer and inner bands ($\Omega = 3{\cdot}32$ less than and close to $\Omega_{cr}^{\alpha(3:1)}$ and $\Omega_{cr}^{\beta(6:1)}$).

6. NUMERICAL EXPERIMENTATION

For numerical simulations of resonance-characterized chaotic motion in the separatrix band, a second order symplectic scheme [26, 27] is used with time step $\Delta t = 10^{-6}$–$10^{-7}\,T$, where $T = 2\pi/\Omega$, and a precision of 10^{-8}. When $\alpha_1 = \alpha_2 = 1{\cdot}0$ and $Q_0 = 0{\cdot}05$, the chaotic motion in the generic separatrix band are generated through 20 000 Poincaré mappings of equation (1), as illustrated in Figure 7 for $\Omega = 1{\cdot}65, 2{\cdot}45, 2{\cdot}7, 3{\cdot}32$. In Figure 7(a), the chaotic motion in the separatrix band is characterized by the (2:1) outer resonance owing to $\Omega = 1{\cdot}65 < \Omega_{cr}^{\beta(2:1)} \approx 1{\cdot}67$. However, all the other resonances are submerged in the separatrix band because $Q_0 = 0{\cdot}05 \gg Q_0^{cr}$ for $\Omega = 1{\cdot}65$. With increasing Ω over $\Omega_{cr}^{\beta(2:1)} \approx 1{\cdot}67$ for specified excitation, the (2:1)-outer resonance will not exist in the separatrix band. Therefore, in Figure 7(b) at $\Omega = 2{\cdot}45$, it is observed that the (2:1)-inner resonance and (4:1)-outer resonance are embedded in the separatrix because this excitation frequency is less than and close to $\Omega_{cr}^{\alpha(2:1)} \approx 2{\cdot}5$ compared to $\Omega_{cr}^{\beta(4:1)} \approx 2{\cdot}8$. The (4:1)-outer resonant separatrix is partially destroyed by its own sub-resonance, and its own width become thicker. However, the (2:1)-inner resonant separatrix is relatively thin. When Ω further increases over $\Omega_{cr}^{\alpha(2:1)}$, the (2:1)-inner resonance will disappear. Therefore, for $\Omega = 2{\cdot}7$, only the outer (4:1)-resonance is in the generic separatrix band, as shown in Figure 7(c). That is because $\Omega = 2{\cdot}7 > \Omega_{cr}^{\alpha(2:1)}$ and $\Omega = 2{\cdot}7 < \Omega_{cr}^{\beta(4:1)}$. It is clearly observed that the width of the (4:1)-outer resonant separatrix becomes thinner compared to the one in Figure 7(b). When $\Omega = 3{\cdot}32$ is less than and close to $\Omega_{cr}^{\alpha(3:1)} \approx 3{\cdot}35$ and $\Omega_{cr}^{\beta(6:1)} \approx 3{\cdot}55$ is used for simulations, the (3:1)-inner and (6:1)-outer resonances are involved in the separatrix band, which is clearly shown in Figure 7(d). From the above numerical simulations, the separatrix bandwidth becomes smaller when the lower order resonance disappears in the separatrix band with increasing excitation frequency for a specified excitation strength.

7. CONCLUSION

The resonant characterization of chaotic motions in the generic separatrix band of the Mathieu–Duffing oscillator is investigated. The resonant conditions for such an oscillator are obtained, and the resonant orders inside and outside the generic separatrix are $(M{:}1)$ and $(2M{:}1)$ respectively. Based on the resonant conditions, the analytical conditions for prediction of the onset of such a specific resonance in the separatrix band are developed through the accurate standard mapping and incremental energy approaches. However, the incremental energy approach gives a very good prediction compared to the numerical predictions. In addition, the bandwidth is computed and it is strongly dependent on the resonance. The stability based on the linearized equation or linear Mathieu equation may not exist for such a Mathieu–Duffing oscillator with a twin-well potential. These results are applicable for post-buckled structures.

REFERENCES

1. A. H. NAYFEH and D. T. MOOK 1979 *Nonlinear Oscillations*. New York: John Wiley and Sons.
2. G. DUFFING 1981, *Erzwungene Schwinggungen bei Veranderlicher Eigenfrequenz*. Braunchweig: Vieweg.
3. L. E. REICHL and W. M. ZHENG 1984 *Physical Review* **29A**, 2186–2193. Field-induced barrier penetration in the quadratic potential.
4. L. E. REICHL and W. M. ZHENG 1984 *Physical Review* **30A**, 1068–1077. Perturbed double-well system: the pendulum approximation and low-frequency effect.
5. B. V. CHIRIKOV 1979 *Physics Report* **52**, 263–379. A universal instability of many-dimensional oscillator systems.

6. D. F. ESCANDE 1985 *Physics Report* **121**, 165–261. Stochasticity in classic Hamiltonian systems: universal aspects.
7. A. C. J. LUO and R. P. S. HAN 1999 *Journal of Sound and Vibration* **227**, 523–544. Analytical predictions of chaos in a nonlinear rod.
8. A. C. J. LUO, K. GU and R. P. S. HAN 1999 *Nonlinear Dynamics* **19**, 37–48. Resonant-separatrix webs in stochastic layers of the twin-well Duffing oscillator.
9. A. C. J. LUO 2001 *Journal of Sound and Vibration* **240**, 821–836. Resonant overlap phenomena in stochastic layers of nonlinear Hamiltonian systems with periodic excitations.
10. A. C. J. LUO and R. P. S. HAN 2001 *Chaos, Solitons and Fractals* **12**, 2493–2508. A resonant theory for stochastic layers in nonlinear dynamic systems.
11. E. SEVIN 1961 *American Society of Mechanical Engineers Journal of Applied Mechanics* **28**, 330–334. On the parametric excitation of pendulum-type vibration absorber.
12. C. S. HSU 1963 *American Society of Mechanical Engineers Journal of Applied Mechanics* **30**, 369–372. On the parametric excitation of a dynamics system having multiple degrees of freedom.
13. C. S. HSU 1965 *American Society of Mechanical Engineers Journal of Applied Mechanics* **32**, 373–377. Further results on parametric excitation of a dynamics system.
14. W. K. TSO and T. K. CAUGHEY 1965 *American Society of Mechanical Engineers Journal of Applied Mechanics* **32**, 899–902. Parametric excitation of a nonlinear system.
15. M. MOND, G. CEDERBAUM, P. B. KHAN and Y. ZARMI 1993 *Journal of Sound and Vibration* **167**, 77–89. Stability analysis of non-linear Mathieu equation.
16. R. S. ZOUNES and R. H. RAND 2000 SIAM *Journal of Applied Mathematics* **58**, 1094–1115. Transition curves for the quasi-periodic Mathieu equations.
17. C. A. TAN and B. KANG 2000 in *Dynamics, Acoustics and Simulations* (Han, R. P. S., Less, K. H., Luo, A. C. J., editors), ASME DE-Vol. 108, 277–282. Dynamics of a nonlinear system under combined parametric and quasi-periodic excitation.
18. A. J. LICHTENBERG and M. A. LIEBERMAN 1992 *Regular and Chaotic Dynamics*. New York: Springer-Verlag; second edition.
19. L. E. REICHL 1992 *The Transition to Chaos in Conservative Classic System: Quantum Manifestations*. New York: Springer-Verlag.
20. J. M. GREENE 1968 *Journal of Mathematical Physics* **9**, 760–768. Two-dimensional measure-preserving mappings.
21. J. M. GREENE 1979 *Journal of Mathematical Physics* **20**, 1183–1201. A method for computing the stochastic transition.
22. H. POINCARÉ 1890 *Acta Mathematica* **13**, 1–271. Sur la probleme des trois corps et les equations de la dynamique.
23. V. K. MELNIKOV 1962 *Soviet Mathematics-Doklady* **3**, 109–112. On the behavior of trajectories of system near to autonomous Hamiltonian systems.
24. V. K. MELNIKOV 1963 *Transactions Moscow Mathematics Society* **12**, 1–57. On the stability of the center for time periodic perturbations.
25. V. I. ARNOLD 1964 *Soviet Mathematics-Doklady* **5**, 581–585. Instability of dynamical systems with several degrees of freedom.
26. K. FENG and M. Z. QIN 1991 *Computational Physical Communication* **65**, 173–187. Hamiltonian algorithms for Hamiltonian systems and a comparative numerical study.
27. R. MCLACHLAN and P. ATELA 1992 *Nonlinearity* **5**, 541–562. The accuracy of symplectic integrators.